CHARACTERIZATION OF COPPER NANORODS USING MOLECULAR DYNAMICS SIMULATIONS

D. Milani, *NTNU Nanomechanical Lab*

ABSTRACT: Mechanical properties of metal nanorods are very important for design and fabrication of Nanoelectromechanical components. A study about the elastic properties of copper nanorods is presented; a series of numerical simulations on different models has been conducted, showing the changes in the characteristcs of the material in different conditions. In particular the changes in Young's modulus have been investigated. The fundamental instrument for the analysis is the stress-strain curve derived from the numerical model: from this it is possible to obtain the main parameters of copper. First of all some test at different temperatures have been conducted. It has been noticed that increasing the temperature, the Young's modulus decreases with a linear trend. Then changes depending on the size of the cross section of the rod and on the strain rate are discussed in detail. Particular attention was also given to the phenomenon of ductile fracture and the yield stress, focusing on the phenomenon of dislocations.

---

1 Introduction

With the fast advance of nanotechnology, metal nanorods and nanowires have received more and more attention. Nanoechanicals systems are evolving, with new scientific studies and technical applications emerging. Mechanical devices are shrinking in thickness and width to reduce mass (e.g. MEMS, NEMS): metal nanorod and nanowires are important components of nanoscale devices. Computational techniques based on Molecular Dynamics (MD) simulations of the representative atomistic configuration of the metallic nanorods provide an effective means of understanding the mechanical deformation behavior of these nanocomponents.

In this work some numerical tests concerning nanorods subjected to a tensile stress have been performed. The behavior of the material at the atomic level is very different from the macroscopic case: at this scale it is crucial to consider the direction in which the specimen is stressed; in addition the effect of the slip of the dislocations is clearly visible. MD techniques help us in this survey; however, it is necessary to set up a precise model, with the appropriate boundary conditions, thermodynamic variables and the applied load.

Another important parameter is the type potential used during the simulations. It is essential for describing the interactions between the atoms. In the current article the approximation of the potential with the Embedded Atom Model (EAM) has been adopted, which provides more stable results than the Lennard-Jones potential [1].

From numerical simulation it is possible to extrapolate the curve stress-strain. It is the basis for the discussion of the mechanical parameters under consideration. To plot this curve the data from the output files have been used. As regards the calculation of the stress at the atomic level, the generic component of the tensor is given by

$$p_{ij} = \frac{\sum_k^N m_k v_{ki} v_{kj}}{V} + \frac{\sum_k^N r_{ki} f_{kj}}{V} \tag{1.1}$$

which comes from the Virial Theorem. The computational software uses virial stress to describe the macroscopic (continuum) stress in accordance with the microscopic quantities [1].

The nanorod is loaded with a tensile stress in the z direction, parallel to the $[001]$ direction of the copper structure. The values of the components of the stress tensor are given as output and thus they can be directly utilized.

Concerning the deformation, it can be derived from the length of the box referred to during the simulation. According to the definition:

$$\varepsilon_{zz} = \frac{L_z - L_{z0}}{L_{z0}} \tag{1.2}$$

as the deformation that affects these tests is related to the z direction.

It is therefore possible to plot a stress-strain curve, similar to the one shown in Figure 1.1, which is evaluated for a copper nanorod at $T = 10\,K$, and final strain $\varepsilon_{zz} = 0.5$.

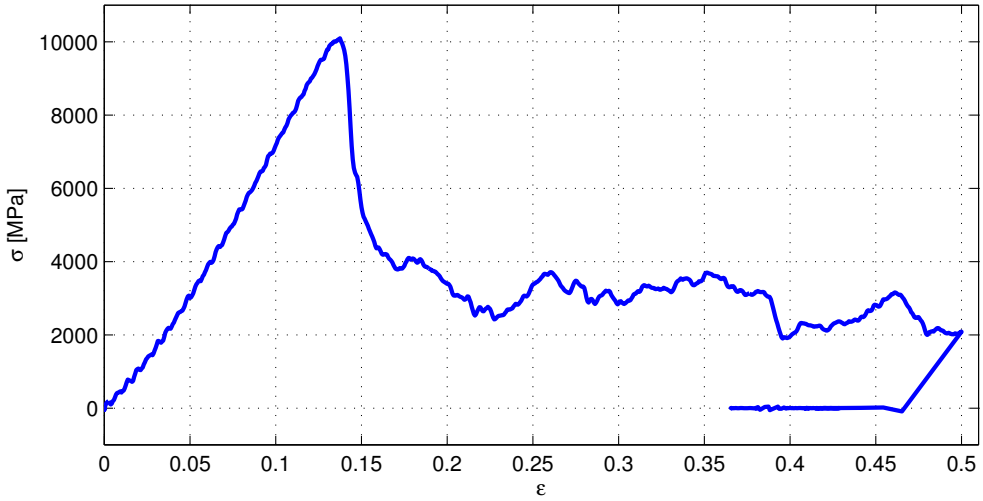

Figure 1.1: $\sigma - \varepsilon$ curve, for $T = 10\,K$, $\varepsilon_{max} = 0.5$

2 Method

For each simulation two input scripts have been prepared. With the first the equilibrium of the structure is processed, with the second the proper load test takes place.

The nanorod is built using the function *box*, which provides for the setting up of single crystal copper according to a *fcc* (face-centered cubic) crystal lattice. On the structure periodic boundary conditions are imposed along the z direction. The next step is the energy minimization, in order to find the disposition of atoms at the given temperature. To do this the Isobaric-Isothermal Ensemble (NPT) is adopted: this ensemble is characterized by a fixed number of atoms N, fixed pressure P, and a fixed temperature T.

The results from this first script serve as input to a second, which make a further equilibration, achieved through a Canonical Ensemble or NVT (the thermodynamic state of the system is characterized by a fixed number of atoms N, fixed volume V, and at fixed temperatures T).

After this the specimen is loaded. The test is accomplished by imposing a deformation of the crystal lattice up to a preset maximum value. At the end the load is removed, and a phase of free relaxation takes place, according to the NPT ensemble [2].

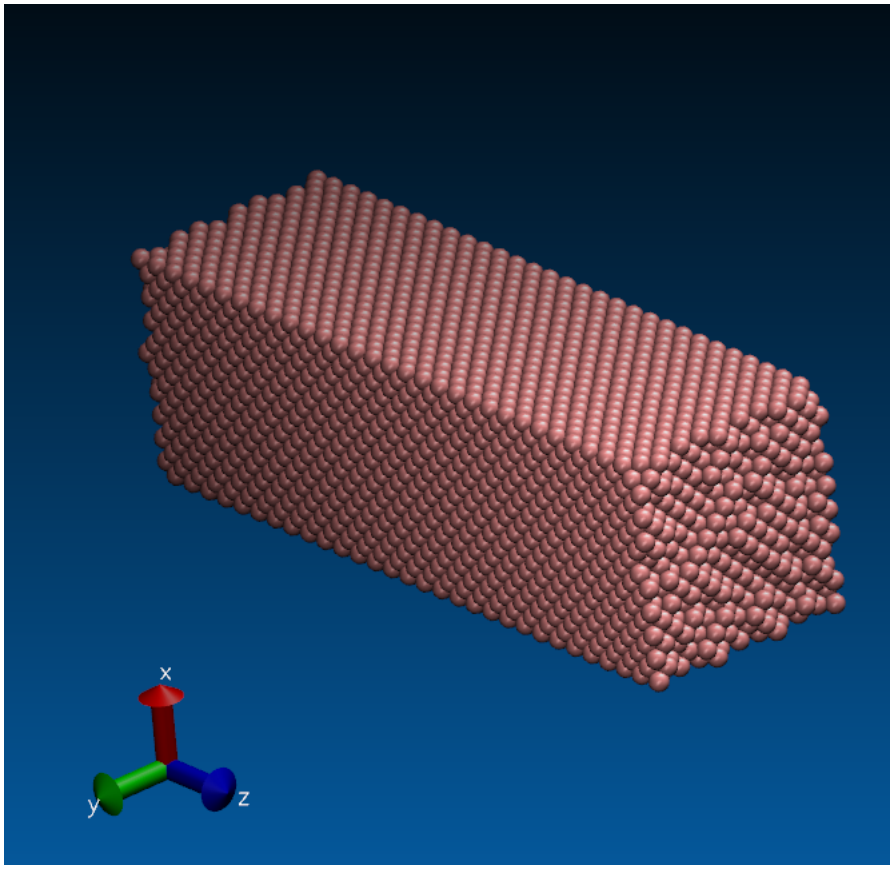

Figure 2.1: The initial configuration of molecular dynamics simulation for the tensile test

All simulations have beenperformed with a timestep of $1\,fs$. As useful addition to the main thermodynamic quantities of data processing, trajectories of individual atoms are given as ouptut, which can be used to graphically display the behavior of the system.

The situation of uniaxial tensile load is recreated by imposing strain applied in the [001] direction of the copper lattice, as shown in Figure 2.1.

For the computational processes the software LAMMPS (Large-scale Atomic/Molecular Massively Parallel Simulator) has been used, a Molecular Dynamics program from Sandia National Laboratories. It is based on MPI protocol and it is a free and open source software. The simulations have been performed in a LAMMPS - OpenMPI environment, compiled on a computer equipped with GNU/Linux operating sistem (Ubuntu 11.10, Kernel 3.0.0-14, 64 bit).

For the visualization of the results, the VMD (Visual Molecular Dynamics) software has been employed, that is a notable tool for viewing the results of the simulations.

For the processing of data several scripts in MATLAB language have been written, which lends itself well to the collection and computing of a large amount of information coming from the numerical simulations.

The software is well suited to parallel computing; therefore the hardware adopted for the Molecular Dynamics computation is an Intel Core 2 Duo CPU working at the frequency of 2.40 Ghz; since the multithreading allows tangible benefits in terms of computational time, both cores have been used. For the VMD visualization a NVIDIA GeForce graphic card was used, in order to accelerate graphics processing (with CUDA architecture support).

---

3 Results

Once the output data are collected from LAMMPS, it is possible to plot the stress-strain relation, according to the relationships described by Equation 1.1 and Equation 1.2. As a example in the Figure 3.1 the curve for values of $T = 10\,K$ and $\varepsilon_{zz} = 0.5$ is shown.

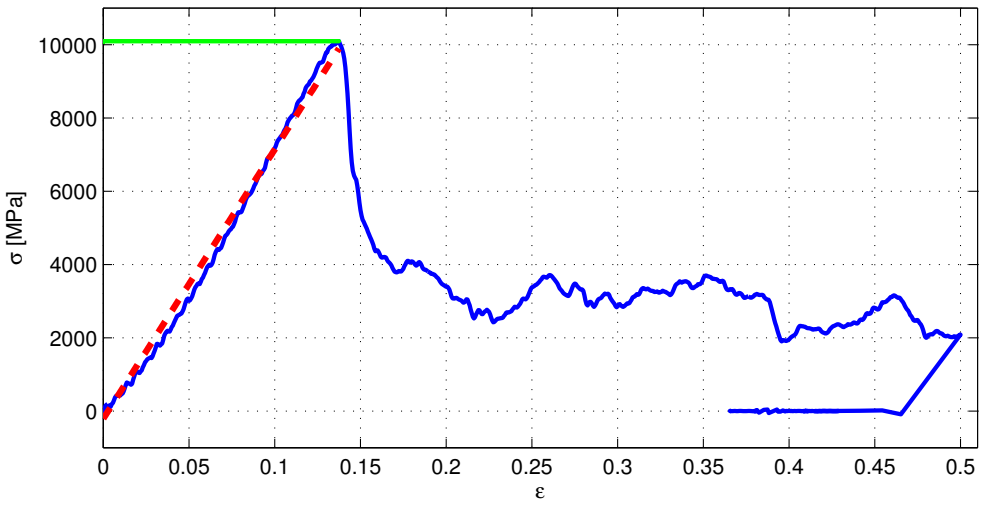

Figure 3.1: $\sigma - \varepsilon$ curve for $T = 10\,K$, $\varepsilon_{max} = 0.5$, with linear regression for Young's modulus estimation and yielding stress peak

The stress increases initially with strain and then decreased sharply: the behavior is no longer elastic. The peak point corresponds to the yield strength σ_y [3]. After the first yielding, the elongation deformation proceeds alternating quasi-elastic and yielding stage.

Note that at the final part of the curves, when the load is removed, the deformation decreases, due to the elastic recovery of the material. As shown in Figure 3.1, the first part of the curve can be assumed as linear. To estimate the elastic modulus of the component analyzed the linear regression using the values until the first peak.

3.1 Temperature effect

The first analysis has conducted on specimens subjected to the same maximum strain $\varepsilon_{zz} = 0.5$ by varying the temperature. The stress and strain curves for temperatures $T = 10, 100, 200, 300, 400, 500\,K$ are represented in Figure 3.2. Related to these, the value of the Young's modulus has been also evaluated and reported in Table 1.

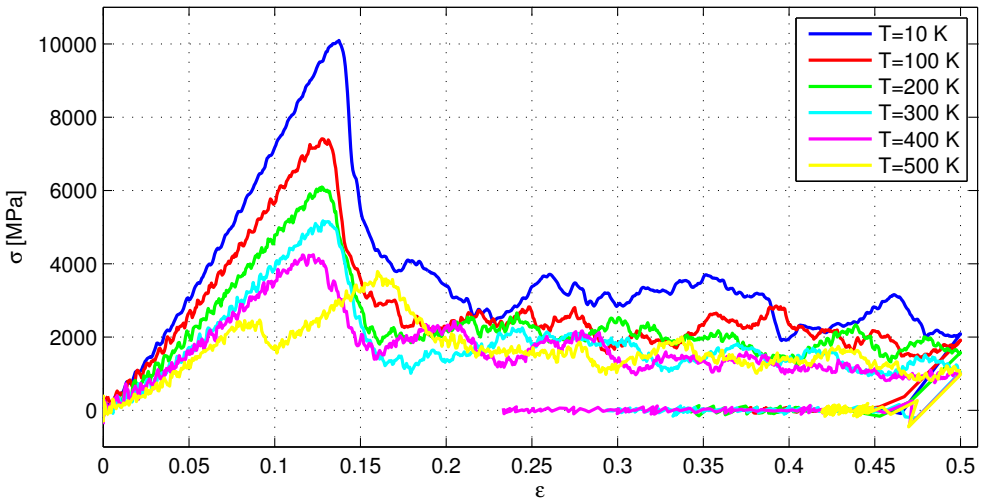

Figure 3.2: Temperature influence on strain-stress curve

$T\,[K]$	$E\,[GPa]$	$\sigma_y\,[GPa]$
10	72.12	10.9
100	57.13	7.41
200	47.31	6.09
300	39.94	5.17
400	34.71	4.25
500	27.70	3.47

Table 1: Young's modulus and yield stress, for tests at different temperatures

The values of Young's moduli are plotted as a function of temperature in Figure 3.3. As it is possible to see they linearly decrease with increasing temperature (which is directly related to the kinetic energy).

The yield stresses at each temperature value are plotted in Figure 3.4 . The numerical values are also collected in Table 1.

As the elastic modulus also the yielding stress decreases approximately linearly with increasing temperature. This is the thermal-softening effect. It is also noteworthy that the above two material constants vary significantly with temperature .

It should be noted also that with the increase of ensemble temperature, the thermal oscillations due to numerical corrections and temperature scaling become dominant [4].

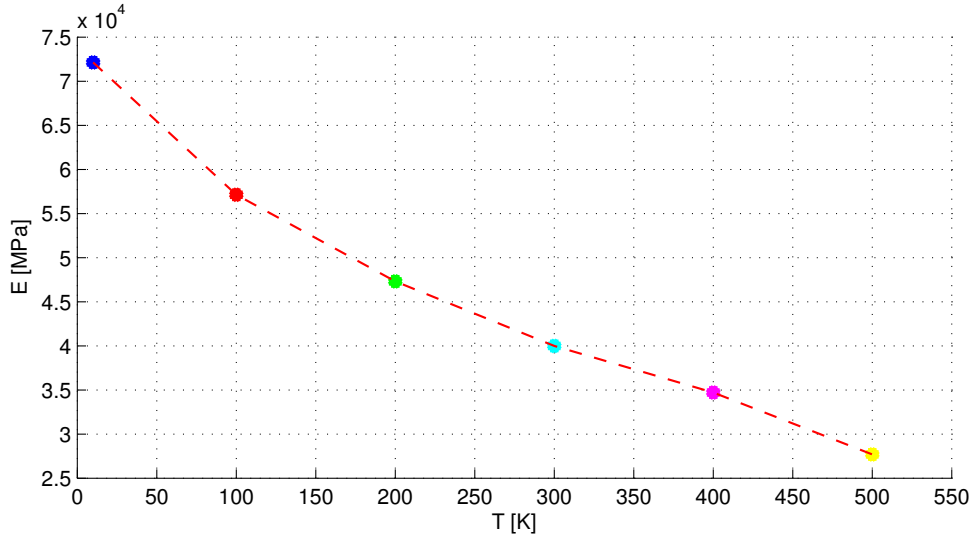

Figure 3.3: Young's modulus as a function of the temperature; the data decrease with a linear trend

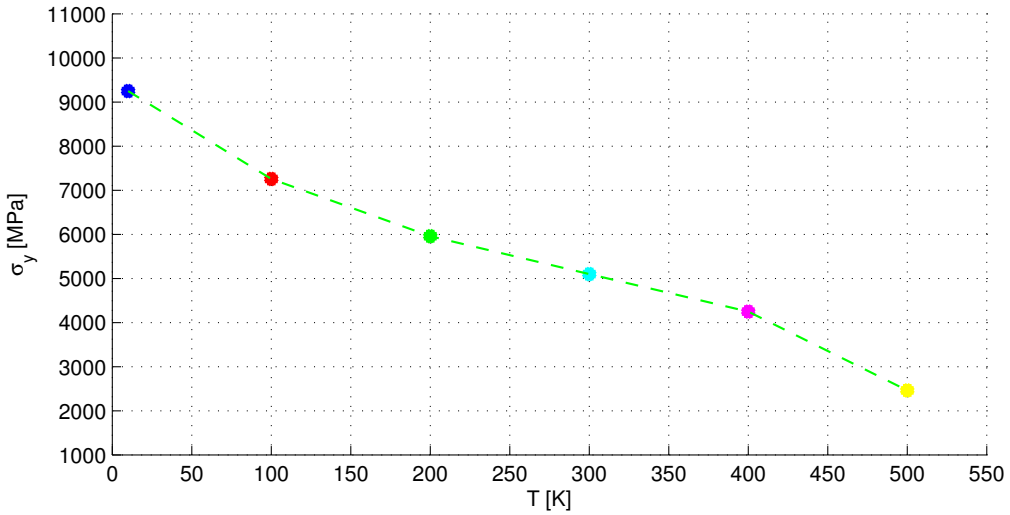

Figure 3.4: Yield stress as a function of the temperature

3.2 Strain rate effect

It is now investigated the effect of strain rate on the elastic modulus and yield stress. The Figure 3.5 representes the $\sigma - \varepsilon$ curves at different strain rates, respectively for $\dot{\varepsilon} = 1 \cdot 10^{11}\, s^{-1}$, $\dot{\varepsilon} = 5 \cdot 10^{10}\, s^{-1}$, $\dot{\varepsilon} = 2.5 \cdot 10^{10}\, s^{-1}$, $\dot{\varepsilon} = 6.25 \cdot 10^{9}\, s^{-1}$.

For all these simulations, the temperature is $T = 10\, K$, while the deformation $\varepsilon = 2$.

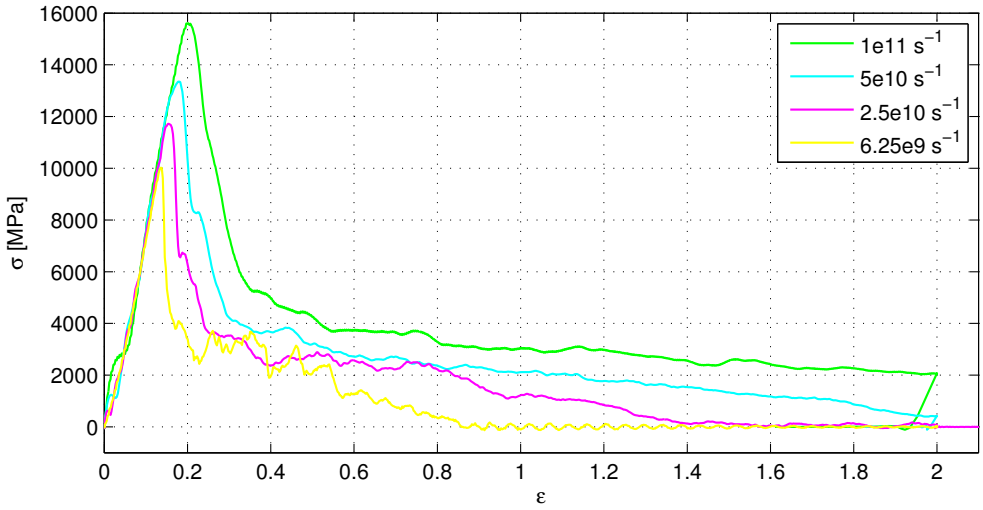

Figure 3.5: Strain rate effect on $\sigma - \varepsilon$ curves

In Figures 3.6 and 3.7 the trends for E and σ_y are shown, by varying the velocity of the application of the load. In Table 2 it is possible to read the numerical values of the variables mentioned above.

$\dot{\varepsilon}\,[s^{-1}]$	$E\,[GPa]$	$\sigma_y\,[GPa]$
$1 \cdot 10^{11}$	78.89	15.6
$5 \cdot 10^{10}$	77.32	13.35
$2.5 \cdot 10^{10}$	75.42	11.72
$6.25 \cdot 10^{9}$	73.32	10.02

Table 2: Young's modulus and yield stress, for tests at different strain rates

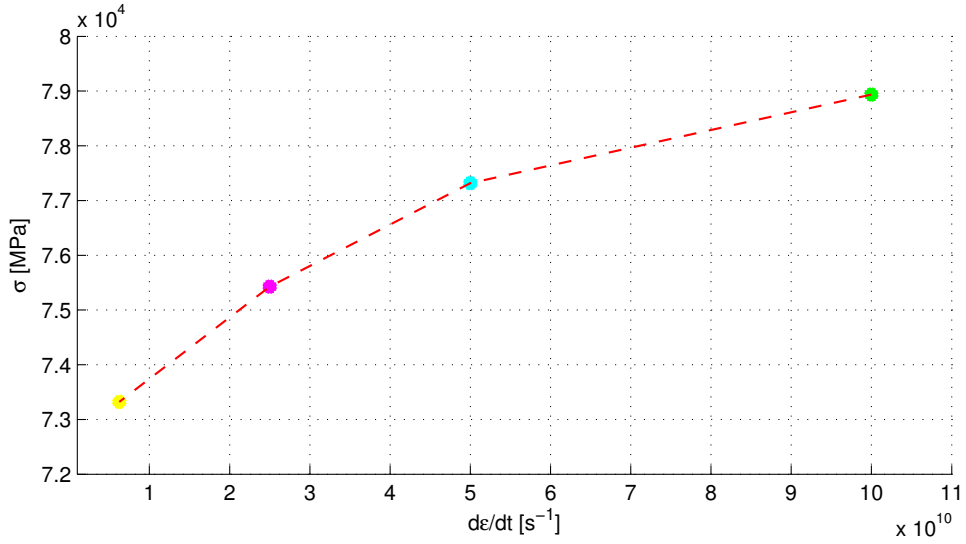

Figure 3.6: Young's modulus as a function of the strain rate

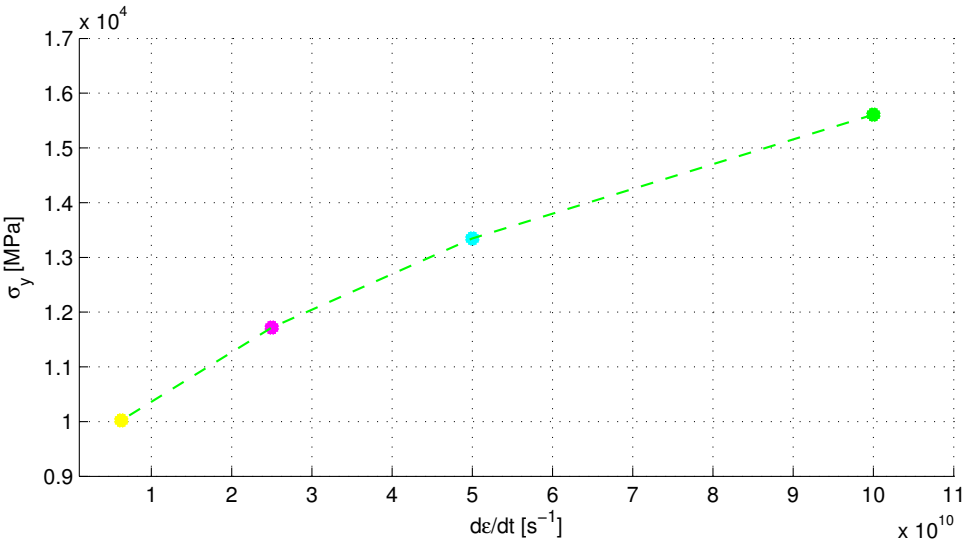

Figure 3.7: Yield stress as a function of the strain rate

Thus the elastic modulus and yield stress of nanorod are dependent on the strain-rates. As the stretch velocity increases, the strain causing the first yield increases too, and the period of yielding is extended [5]. In this case the trend is logarithmic.

Note that unlike in the previous curves, in this case the deformation does not decrease during the free relaxation phase: this can only mean that the nanorod has broken during the deformation (except in the case of highest strain rate).

3.3 Size effect

Finally the influence of geometric parameters of the nanorod has been studied: various tests have been performed with different values of the rectangular section of the nanorod; then the values of E and σ_y are calculated varying the section (side of the square section $4a$, $5a$, $7a$, $9a$, where a is the lattice constant). The aspect ratio between the 3 dimension has been kept constant and equal to 3:3:10. These tests have been conducted at the same temperature $T = 10\,K$ and the maximum strain of $\varepsilon = 0.5$ (Figure 3.8).

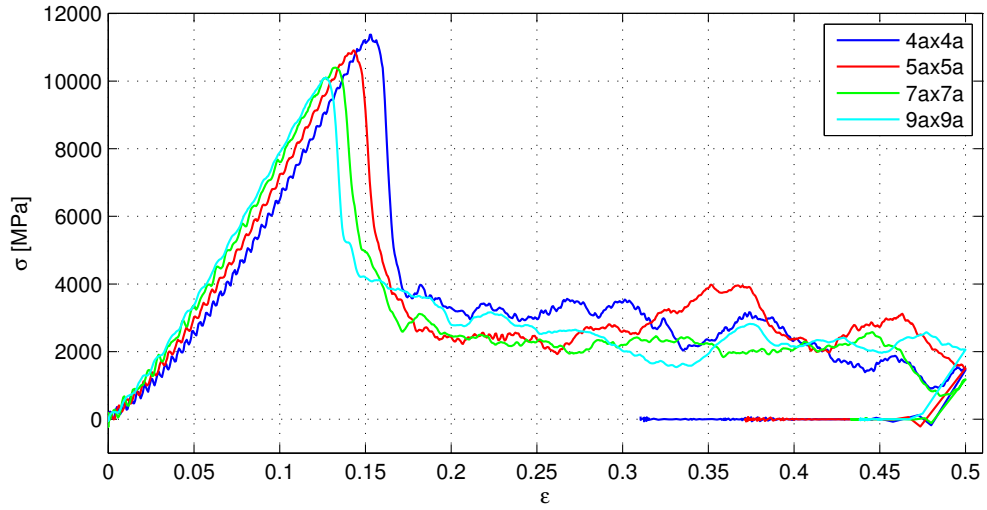

Figure 3.8: $\sigma - \varepsilon$ curves for different cross sections

The Table 3 and Figure 3.9 and 3.10 show the values of Young's modulus and the yield stress, respectively.

$L_x \times L_y$	$E\,[GPa]$	$\sigma_y\,[GPa]$
$4a \times 4a$	71.40	11.37
$5a \times 5a$	74.91	10.91
$7a \times 7a$	78.01	10.40
$9a \times 9a$	79.24	10.10

Table 3: Young's modulus and yield stress, for tests at different cross sections

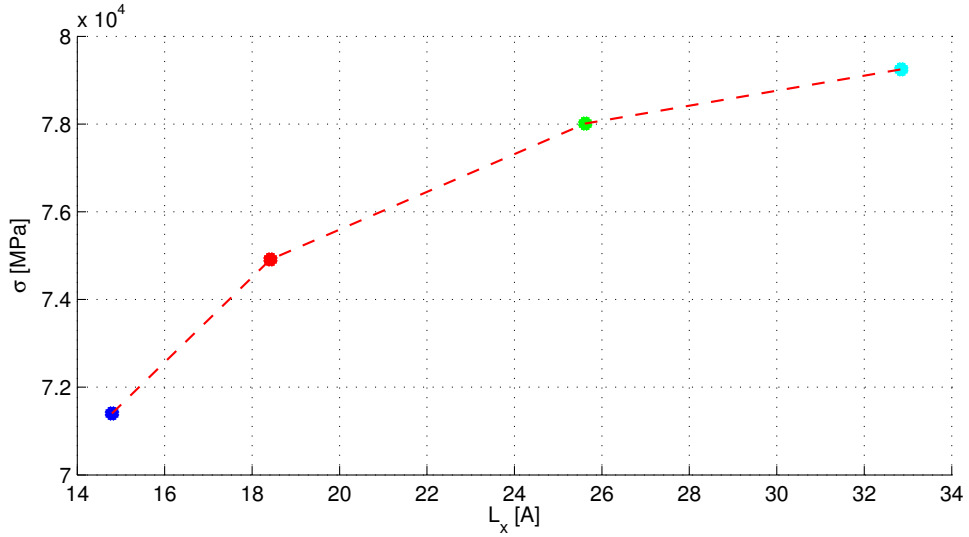

Figure 3.9: Young's modulus for different sections

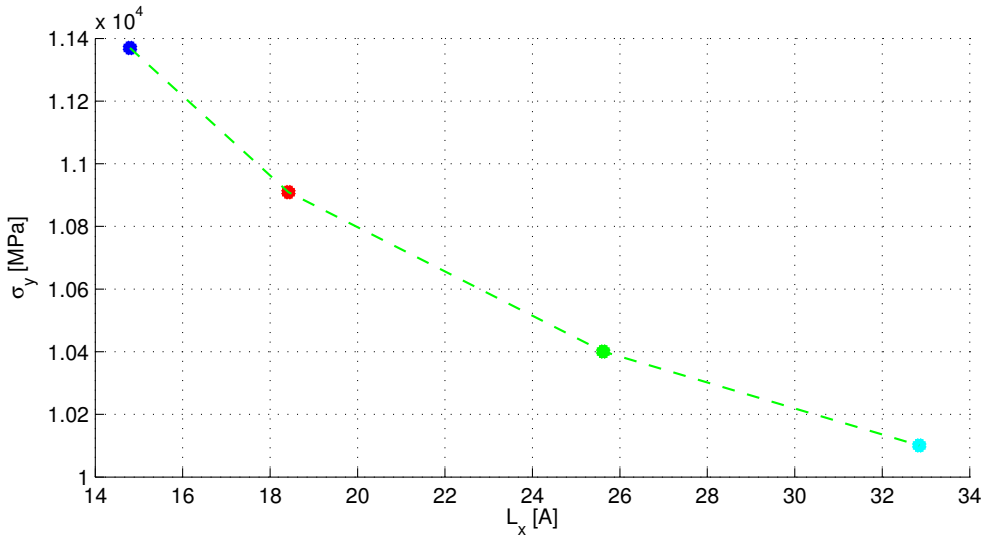

Figure 3.10: Size effect on yield stress

It is found that the mechanical properties of metal nanorod are considerably size-dependent. The elastic modulus increases with increasing size of cross-section, while yielding stress decreases with increasing size of cross-section [3].

4 Discussion and conclusion

The comparisons of Young's modulus at various temperatures are listed in Table 2. As the temperature rises, the Young's modulus of the material linearly decreases since the material has less bonding energy at higher temperatures (that means at higher kinetic energy). Instead for the cross-section and the strain rate the dependence has rather a logarithmic trend.

As it is possible to notice analyzing any stress-strain curve, the deformation before yielding is elastic. After reaching the peak value, the stress goes down dramatically. Then, the stress–strain curve is saw-toothed. The first sharp drop of stress comes from the occurrence of dislocation. The following saw curve comes from the nucleation and movements of the dislocations.

The deformations preferentially take place by slips in {111} planes. The reason is that the {111} planes of Cu are closely packed and have the lowest cohesive energy [6]. Whenever yielding occurs, atomic structure is disordered, the original stacking sequence is deformed, the section get narrowed more and more, and the tensile force decreases abruptly.

In the Figure 4.1 the slip of dislocations is presented. The images refer to a nanorod at $T = 10$ K at $\varepsilon_{zz} = 0.08$ (elastic behavior, no plastic deformation) and $\varepsilon_{zz} = 0.13$ $\varepsilon_{zz} = 0.16$ (before and after the first yield point: it is possible to notice the occurrence of dislocations and then their slip).

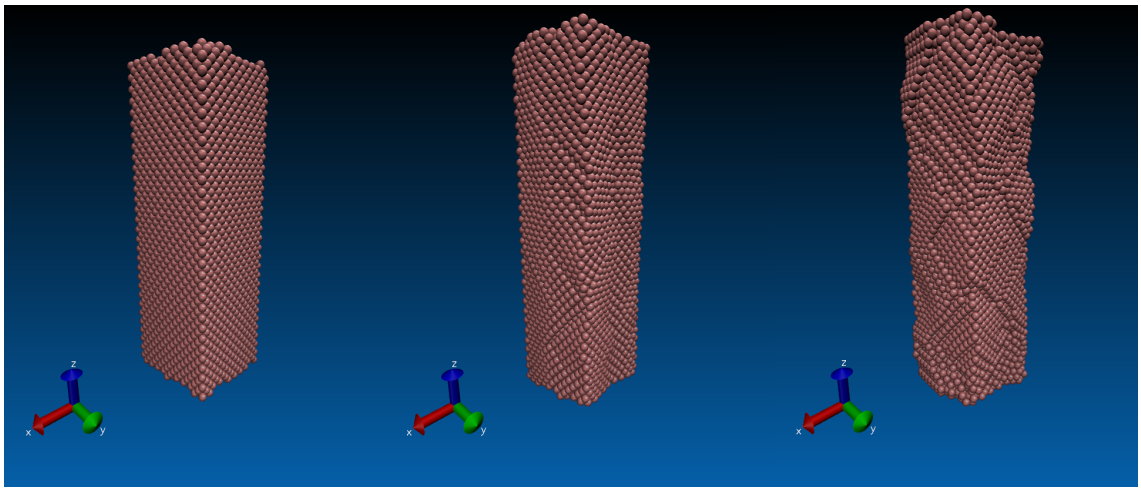

Figure 4.1: Dislocations evolution in the nanorod, for $\varepsilon_{zz} = 0.08$, $\varepsilon_{zz} = 0.10$ and $\varepsilon_{zz} = 0.16$

As noted above from the strain curve, the nanorods subjected to the maximum deformation $\varepsilon = 2$ break. Through the use of VMD it is possible to examine first the occurrence of dislocations (common to all tests, after the yielding point) and then the fracture. As a matter of fact, copper is a typical ductile material, and then the deformation and the racture depend on the nucleation and on the slip of the dislocations [1]. In the Figure 4.2 the sequence of the fracture is shown (nanorod with $6a \times 6a$, at $T = 10\,K$, $\dot{\varepsilon} = 2.5 \cdot 10^{10}\,s^{-1}$); it is easy to recognize the typical ductile fracture.

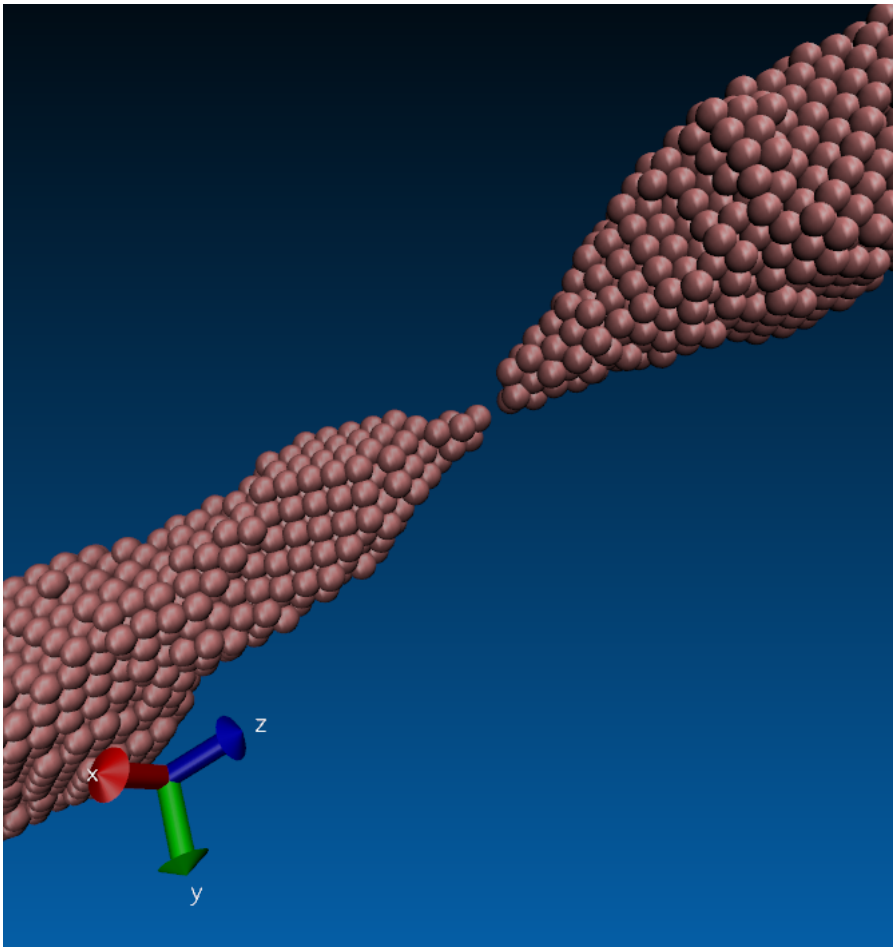

Figure 4.2: Ductile fracture in the nanorod, at $\varepsilon_{zz,frac} = 1.26$

References

[1] Z. Zhang, J. He, S. Nagao, 2011, Lecture notes from Nanomechanics course, NTNU

[2] LAMMPS Manual, http://lammps.sandia.gov

[3] H.A. Wu, *Molecular dynamics study on mechanics of metal nanowire*, Mechanics Research Communications 33 (2006), pp. 9-16

[4] Ram Mohan and Yu Liang, *Tensile and Flexural Deformation of Nickel Nanowires via Molecular Dynamics Simulations*, (2010) Cutting Edge Nanotechnology, Dragica Vasileska (Ed.)

[5] H.A. Wu, *Molecular dynamics study of the mechanics of metal nanowires at finite temperature*, European Journal of Mechanics A/Solids 25 (2006), pp. 370–377

[6] Jeong-Won Kang and Ho-Jung Hwang, *Molecular Dynamics Simulation Study of the Mechanical Properties of Rectangular Cu Nanowires*, Journal of the Korean Physical Society, Vol. 38, No. 6, June 2001, pp. 695-700